

## Contact Resistance in Metal–Molecule–Metal Junctions Based on Aliphatic SAMs: Effects of Surface Linker and Metal Work Function

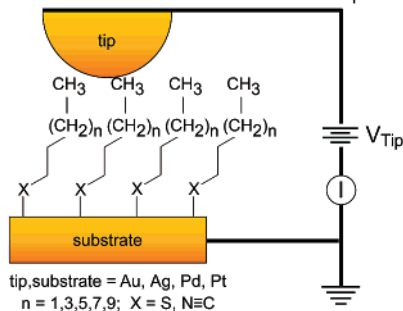
Jeremy M. Beebe,<sup>†</sup> Vincent B. Engelkes,<sup>‡</sup> Larry L. Miller,<sup>†</sup> and C. Daniel Frisbie<sup>\*,‡</sup>

Departments of Chemistry, Chemical Engineering and Materials Science, University of Minnesota, Minneapolis, Minnesota 55455

Received May 8, 2002

Theoretical work on electrical transport in metal–molecule–metal junctions indicates that junction impedance is affected significantly by the properties of the metal–molecule contacts.<sup>1</sup> In particular, the presence of barriers to electron (or hole) injection leads to drops in electrostatic potential at metal–molecule interfaces and thus to contact impedances. With the exception of carbon nanotube-based devices,<sup>2</sup> there have been very few direct measurements of contact effects in molecular junctions.<sup>3</sup> Here we report two terminal, low-voltage contact resistance measurements for molecular tunnel junctions based on self-assembled monolayers (SAMs) of alkane thiols or alkane isonitriles sandwiched between pairs of Au, Ag, Pd, or Pt contacts. We formed the junctions using the conducting probe atomic force microscopy (CP-AFM) approach<sup>4,5</sup> in which a metal-coated AFM tip contacts a SAM on a metal support, Scheme 1. All current–voltage ( $I$ – $V$ ) characteristics were acquired in ambient conditions while controlling the load (2 nN) applied to the tip–SAM microcontact, as previously described.<sup>4</sup> To extract contact resistances ( $R_0$ ), we measured total junction resistance ( $dV/dI|_{V=0}$ ) as a function of the number of CH<sub>2</sub> groups per chain, and extrapolated the resistance to zero CH<sub>2</sub> groups.

### Scheme 1. Schematic Illustration of CP-AFM Experiment



For the purposes of this study, the attractive features of junction formation by CP-AFM are (1) it is experimentally uncomplicated (no nanofabrication steps are necessary) and (2) it is possible to change the metals that contact the SAM. The CP-AFM approach complements a number of alternative junction-forming strategies, such as break junctions,<sup>6</sup> nanopores,<sup>7</sup> SAMFETs,<sup>8</sup> crossed wires,<sup>3c,9</sup> and mercury drop contacts.<sup>10</sup>

Figure 1A,B, shows representative semilog plots of junction resistance versus number of CH<sub>2</sub> groups for alkane thiol (RSH) and alkane isonitrile (RNC) SAMs on Au contacted by an Au-coated tip. For a given alkane chain length, the junction resistance was measured by recording the  $I$ – $V$  characteristic between  $-0.3$

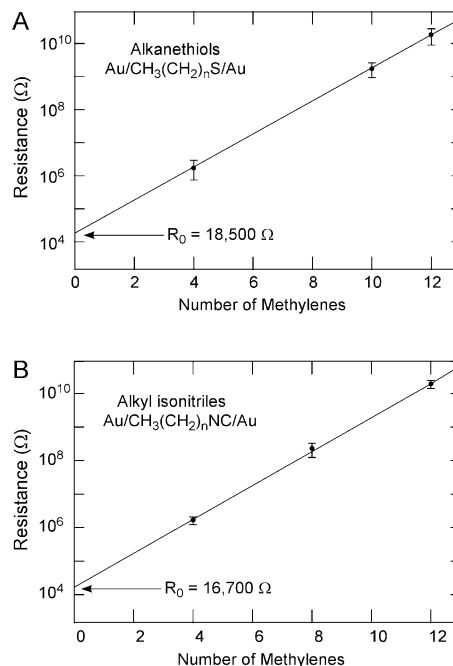


**Figure 1.** Semilog plot of resistance vs alkane chain length for Au/RS/Au junctions (A) and Au/RNC/Au junctions (B). The y-intercept of best-fit line yields the contact resistance,  $R_0$ .

and  $+0.3$  V. Over this voltage range, the  $I$ – $V$  traces were linear and symmetric; five  $I$ – $V$  traces per molecular chain length were used to determine average resistance values. The data shown in Figure 1A,B, were collected with the same Au tip (radius = 100 nm) to avoid complicating the data with variations in tip–SAM contact area that could occur if tips with different radii were used. The plots show that the junction resistance increases exponentially with molecular chain length, as expected for coherent, nonresonant tunneling and in keeping with our previous measurements on alkane thiol SAMs. A best-fit line through the points extrapolated to zero CH<sub>2</sub> groups provides the contact resistance,  $R_0$ .<sup>11</sup> From the extrapolation, we see that the contact resistances for Au/RS/Au and Au/RNC/Au junctions are on the order of 15–20 k $\Omega$  for this specific tip, and the difference between the contact resistances is less than 2 k $\Omega$ . We generally find that  $R_0$  is  $\sim 10\%$  lower for Au/RNC/Au junctions than for Au/RS/Au junctions.

Variation of the type of metal used to contact the SAM has a much bigger effect on  $R_0$ . Figure 2A shows semilog plots of resistance versus length for Au/RS/Au and Ag/RS/Ag junctions, with extrapolated  $R_0$  values of 62 and 234 k $\Omega$ , respectively. The large difference in  $R_0$  for these two junctions motivated us to make systematic measurements of  $R_0$  for alkane thiol junctions with Pd

\* To whom correspondence should be addressed. E-mail: frisbie@cems.umn.edu.

<sup>†</sup> Department of Chemistry.

<sup>‡</sup> Department of Chemical Engineering and Materials Science.

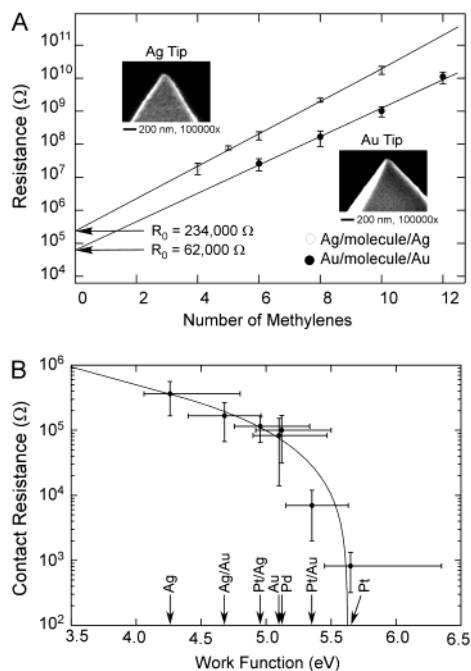


**Figure 2.** (A) Junction resistance vs chain length for alkanethiol junctions with Ag contacts and Au contacts. Solid lines are best-fits. Insets show SEM images of the Ag and Au tips. (B) Contact resistance,  $R_0$ , as a function of metal work functions for alkanethiol junctions. The effective work functions of mixed metal pairs are taken to be the average of the two metal work functions. The solid line is a guide for the eye.

and Pt contacts as well. We made measurements on junctions where the tip metal was the same as the substrate metal and on mixed metal junctions in which the tip and substrate metals were different, for example, tip metal = Au and substrate metal = Pt. Figure 2B is a plot of  $R_0$  versus metal work function resulting from these measurements. Each data point represents an average  $R_0$  and standard deviation determined from resistance versus length plots for 5–10 individual tips. For junctions composed of only one metal, we have used literature values<sup>12</sup> for the metal work function. For mixed metal junctions, we have used the average of the two metal work functions as the effective work function for the contacts. The clear trend shown in Figure 2B is that  $R_0$  decreases with increasing metal work function.

An important additional observation is that for mixed metal junctions we do not observe a difference in  $R_0$  when the tip metal and substrate metal are reversed. For example,  $R_0$  is the same for Au (tip)/Ag (substrate) contacts and for Ag (tip)/Au (substrate) contacts. Furthermore, we observe symmetric  $I$ – $V$  behavior (at low voltage) for all junctions in this study. These are surprising observations because they suggest that the electrical behavior of the physisorbed tip–CH<sub>3</sub> (top) contact is comparable to the chemisorbed substrate–S (bottom) contact. However, intuition and the recent results of others<sup>3b,c</sup> suggest that there should be real differences in the electrical transport properties of metal–S and metal–CH<sub>3</sub> contacts. We emphasize that our contact resistance measurements have been obtained in the low-voltage regime; significant differences between metal–S and metal–CH<sub>3</sub> contacts might not arise until larger voltages are reached. In future experiments, we will address the dependence of contact resistance on applied bias.

Our measurements confirm the importance of metal type to contact resistance in SAM-based molecular junctions as predicted by theory,<sup>1c</sup> and they have important implications for the description of electrical transport. The existence of contact resistance implies

the presence of a barrier to charge transport at the metal–molecule interfaces. The dependence of the contact resistance on the metal type (Figure 2B) indicates that the barrier height decreases with increasing metal work function. Such data should be interpretable in terms of interface dipoles and the Fermi level position ( $E_F$ ) within the HOMO–LUMO gap of the molecules. A precise understanding of the work function dependence of the contact resistance, its relationship to the Fermi level position, and the differences between the metal–S and metal–CH<sub>3</sub> interfaces will require detailed theoretical calculations. However, because high work function contacts (e.g., Pt/Pt) yield smaller barriers, the Figure 2B data are consistent with the conclusion that the Fermi level lies closer to the HOMO than to the LUMO. This means the mechanism of transport in alkane thiol junctions can be referred to appropriately as “hole tunneling.” Cahen and co-workers recently reached a similar conclusion in their studies of transport through aliphatic monolayers contacted with Hg and p-Si electrodes.<sup>10c</sup> Systematic studies of contact resistance versus metal work function have not been reported previously for SAM-based molecular junctions, but they are an important approach to understanding electronic properties of these systems.

In summary, we have demonstrated experimentally that the low-voltage contact resistance in metal–molecule–metal junctions based on aliphatic SAMs has marked dependence on the contact work function. From the work function dependence, we conclude the Fermi level of these junctions lies close to the HOMO. We have also shown that there is a small but measurable difference (~10%) in the contact resistance associated with junctions based on thiol versus isonitrile surface linkers. We are currently pursuing similar measurements on SAMs of conjugated aromatic molecules.

**Acknowledgment.** C.D.F. thanks NSF and the Packard Foundation for financial support.

## References

- (1) (a) Datta, S.; Tian, W.; Hong, Seunghun, Hong; Reifenberger, R.; Henderson, J. I.; Kubiak, C. P. *Phys. Rev. Lett.* **1997**, *79*, 2530–2533. (b) Xue, Y.; Datta, S.; Ratner, M. A. *J. Chem. Phys.* **2001**, *115*, 4292–4299. (c) Seminario, J. M.; De La Cruz, C. E.; Derosa, P. A. *J. Am. Chem. Soc.* **2001**, *123*, 5616–5617.
- (2) Appenzeller, J.; Martel, R.; Avouris, P.; Stahl, H.; Lengeler, B. *Appl. Phys. Lett.* **2001**, *78*, 3313–3315.
- (3) (a) Zhou, C.; Deshpande, M. R.; Reed, M. A.; Jones, L., II; Tour, J. M. *Appl. Phys. Lett.* **1997**, *71*, 611–613. (b) Cui, X. D.; Primak, A.; Zarate, X.; Tomfohr, J.; Sankey, O. F.; Moore, A. L.; Moore, T. A.; Gust, D.; Harris, G.; Lindsay, S. M. *Science* **2001**, *294*, 571–574. (c) Kushmerick, J. G.; Holt, D. B.; Yang, J. N.; Moore, M. H.; Shashidhar, R. *Phys. Rev. Lett.* Submitted for publication.
- (4) (a) Wold, D. J.; Frisbie, C. D. *J. Am. Chem. Soc.* **2000**, *122*, 2970–2971. (b) Wold, D. J.; Frisbie, C. D. *J. Am. Chem. Soc.* **2001**, *123*, 5549–5556. (c) Wold, D. J.; Haag, R.; Rampi, M. A.; Frisbie, C. D. *J. Phys. Chem. B* **2002**, *106*, 2813–2816.
- (5) (a) Cui, X. D.; Zarate, X.; Tomfohr, J.; Sankey, O. F.; Primak, A.; Moore, A. L.; Moore, T. A.; Gust, D.; Harris, G.; Lindsay, S. M. *Nanotechnology* **2002**, *13*, 5–14. (b) Son, K. A.; Kim, H. I.; Houston, J. E. *Phys. Rev. Lett.* **2001**, *86*, 5357–5360. (c) Fan, F.-R. F.; Yang, J.; Cai, L.; Price, D. W., Jr.; Dirk, S. M.; Kosynkin, D. V.; Yao, Y.; Rawlett, A. M.; Tour, J. M.; Bard, A. J. *J. Am. Chem. Soc.* **2002**, *124*, 5550–5560.
- (6) (a) Park, H.; Park, J.; Lim, A.; Anderson, E. H.; Alivisatos, A. P.; McEuen, P. L. *Nature* **2000**, *407*, 57–60. (b) Reed, M. A.; Zhou, C.; Muller, C. J.; Burgin, T. P.; Tour, J. M. *Science* **1997**, *278*, 252–254.
- (7) Chen, J.; Reed, M. A.; Rawlett, A. M.; Tour, J. M. *Science* **1999**, *286*, 1550–1552.
- (8) Schön, J. H.; Meng, H.; Bao, Z. *Nature* **2001**, *413*, 713–716.
- (9) Collier, C. P.; Wong, E. W.; Belohradský, M.; Raymo, F. M.; Stoddart, J. F.; Kuekes, P. J.; Williams, R. S.; Heath, J. R. *Science* **1999**, *285*, 391–394.
- (10) (a) Slowinski, K.; Chamberlain, R. V., II; Bilewicz, R.; Majda, M. *J. Am. Chem. Soc.* **1996**, *118*, 4709–4710. (b) Holmlin, R. E.; Ismagilov, R. F.; Haag, R.; Mujica, V.; Ratner, M. A.; Rampi, M. A.; Whitesides, G. M. *Angew. Chem., Int. Ed.* **2001**, *40*, 2316–2320. (c) Selzer, Y.; Salomon, A.; Cahen, D. *J. Am. Chem. Soc.* **2002**, *124*, 2886–2887.
- (11) Data are fit to the equation:  $\ln(R) = \ln(R_0) + \beta n$ , where  $\beta$  is the structure-dependent factor. Fit gives  $\beta = 1.15/\text{CH}_2$ .
- (12) Michaelson, H. B. *J. Appl. Phys.* **1977**, *48*, 4729–4733.

JA0268332